PROCEEDINGS OF SCIENCE

Development of PPD: characterization and simulation

T. Murase[*a], **H. Oide**[a], **H. Otono**[a], **S. Yamashita**[b]
[a]*Department of Physics, University of Tokyo*
[b]*International Center for Elementary Particle Physics (ICEPP), University of Tokyo*
On behalf of KEK Detector Technology Project
7-3-1 Hongo, Bunkyo, Tokyo, Japan, 113-0033

E-mail: murase@icepp.s.u-tokyo.ac.jp oide@icepp.s.u-tokyo.ac.jp
otono@icepp.s.u-tokyo.ac.jp satoru@icepp.s.u-tokyo.ac.jp

Study of noise of Multi-Pixel Photon Counter (MPPC) produced by Hamamatsu Photonics K.K. (HPK) gives us useful information for developing Pixelated Photon Detector (PPD) with suppressed noise. We investigate its dark noise, after-pulse, and crosstalk separately at a high operational voltage. A Monte-Carlo simulation based on the inner structure and physics of the PPD is performed to investigate its observable characteristics. We report on the current status of the application of a 3D device simulator (TCAD) to the development of PPD. We reproduce some basic characteristics of the MPPC using TCAD and examine the potential of this simulator for use in development of the next-generation PPD.

International Workshop on New Photon Detectors PD09
June 24-26 2009
Shinshu University Matsumoto Japan

[*]Speaker.

© Copyright owned by the author(s) under the terms of the Creative Commons Attribution-NonCommercial-ShareAlike Licence.

PoS(PD09)003

1. Introduction

Pixelated Photon Detector (PPD) is the generic name for the semiconductor photodetectors consisting of an array of Avalanche Photodiodes (APDs) operating in Geiger-mode. Multi-Pixel Photon Counter (MPPC) is a PPD produced by Hamamatsu Photonics K.K. (HPK). These devices are promising for use in future collider experiments in that they can count the number of photons starting from a single photon. For this purpose, we must improve the following: the scalability, the gain, and the maximum photon count per chip. The reduction of noise plays a key role in achieving these goals. The inner mechanism of the MPPC and the physics behind it needs to be understood. In addition, we use a device simulator called Technology CAD (TCAD), which takes into account the semiconductor process as well as its detailed operation in terms of the charge carriers. In this paper, we report the results obtained from the noise measurements of the MPPC and the potential of using TCAD for the future development of PPD.

2. Measurement of Noise

In order to characterize the noise in the MPPC, we measure the different noise components separately. Our measurement setup is shown in Figure 1. The measurement was done for 1600 pixels MPPC [S10362-11-025] produced by HPK [1]. The setup was put into a light shielding box (dark box), so that all triggered pulses were essentially due to the MPPC noise. The measurement was carried out at room temperature (300 K). The digital oscilloscope was used for data storage. Using the time-structure and the pulse-height from the recorded waveforms, the three noise components were separated off-line [2].

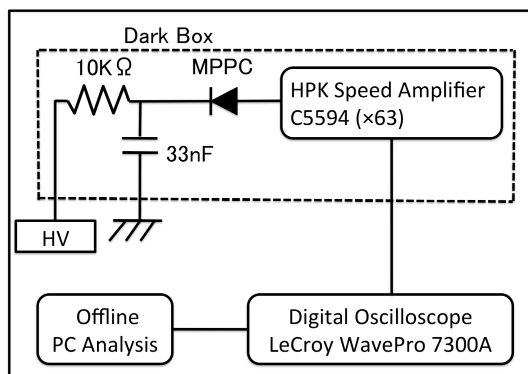

Figure 1: Setup of noise measurement.

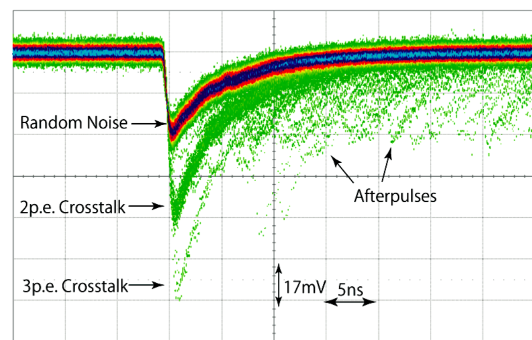

Figure 2: Raw waveform MPPC measured by oscilloscope, persisted for 10s.

Figure 2 shows the dark noise. Its shape can be understood in terms of three different sources. The first is the primary pulse due to the random noise, which consists mostly of thermal fluctuation. Its pulse shape is seen as the dominant feature in Figure 2 and is shown with a thick band. The peripherals around the primary pulse has two components. The pulses which sit at the same position as the primary pulse are understood as optical crosstalk, in which the avalanching photons leak into neighboring cells, whereby triggering multiple channels simultaneously. The integral nature of the pulses can be clearly seen, corresponding to the number of photoelectrons. The peripherals which

PoS(PD09)003

appear after the primary pulse are the after-pulses, which are echoes of the primary pulse. The three noise sources (random noise, crosstalk, after-pulse) have been measured separately. The analysis procedure is described below.

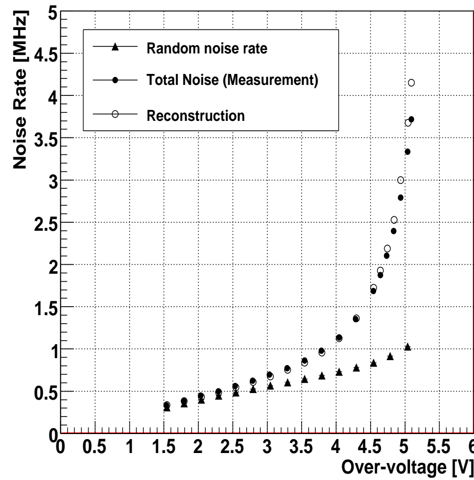

Figure 3: The ΔV dependence of random-noise rate, total noise rate, and reconstruction.

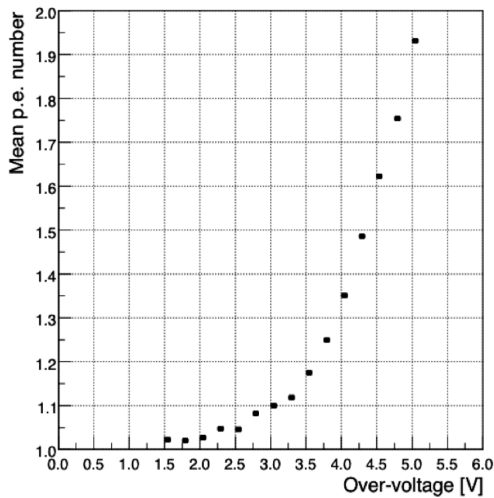

Figure 4: The ΔV dependence of the mean p.e. number for crosstalk.

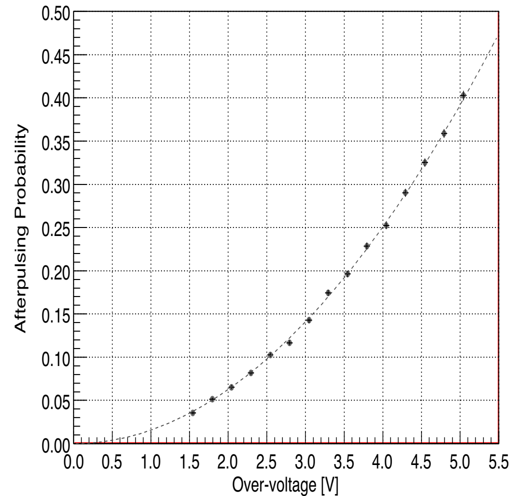

Figure 5: The probability to find after-pulses in next arriving pulses as a function of over-voltage.

2.1 Total noise and random noise rate

The total noise rate was measured by counting the number of triggered pulses with a minimum dead time of the system (13.5 ns). The random noise rate was measured by setting a veto time of 1000 ns to remove the after-pulses. Figure 3 shows the total and random noise rates as a function of ΔV. We find that the random noise rate increases linearly with ΔV. At higher over-voltage, the total noise rate increases abruptly. This explosive increase of the total noise rate limits the maximum

PoS(PD09)003

operational bias voltage. The difference between the total and random noise rates can be accounted for by the after-pulse and crosstalk.

2.2 Optical crosstalk

Figure 4 shows the mean photo electron (p.e.) number as a function of over-voltage (ΔV) where the mean p.e. number is the mean number of firing pixels per avalanche. The magnitude of the triggered pulse was estimated accurately, excluding the influence of its neighboring pulses such as after-pulses by using our waveform analysis method. Figure 4 shows that the crosstalk generation increases drastically with ΔV.

2.3 After-pulse

The after-pulse is measured from the time interval between one triggered pulse and its next arriving pulse (greater than 10 ns). Waveforms with 1 p.e. triggered pulse that have no preceding pulses during 200 ns before their origination time were selected. Some of the next-arriving pulses are due to random noise pulses, which is a background to the estimation of the after-pulse. The after-pulse can be extracted using the fact that its rate decreases exponentially with increasing arrival time, while the rate remains constant in time for the case of random noise. We also measured the voltage dependence of the after-pulse rate. Figure 5 shows that the after-pulsing probability is proportional to $(\Delta V)^2$.

2.4 Reconstruction

We combine the three noise components which were measured separately, and compare with the measured total noise in Figure 3. We get good agreement between the total noise rate measured inclusively and the combined noise rate calculated from the three noise components. The three noises fully account for the total noise.

2.5 Difference of behavior in ΔV dependence

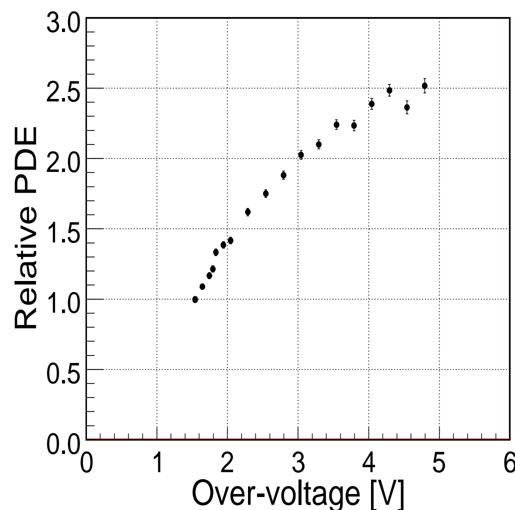

Figure 6: Measurement of relative PDE.

PoS(PD09)003

The measurement of photon detection efficiency (PDE) of MPPC is essential for the development of PPD. We measured the voltage dependence of the PDE using a blue LED of 470 nm wavelength as a light source inside the dark box. Its light was diminished sufficiently so that only single photon reached the MPPC most of the time. Figure 6 shows the result of the voltage dependence of the relative PDE value normalized to the value at V_{op} = 75.0 V (ΔV = 1.55 V). It is observed that the PDE tends to saturate as ΔV increases. Similar results can be seen in Ref. [3]. The saturating behavior of the PDE is a curious feature, not seen in the random noise rate, even though both quantities are rooted in avalanche multiplication. To explain this difference, we performed a simple Monte-Carlo (MC) simulation considering the inner structure of the MPPC.

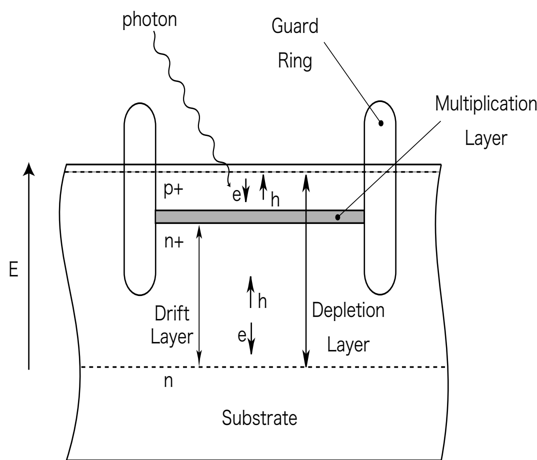

Figure 7: Expected structure of PPD.

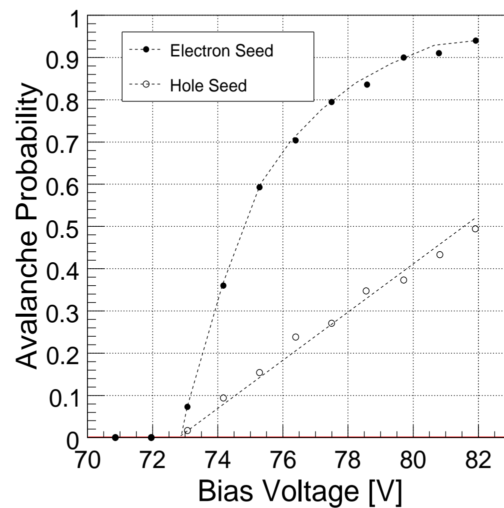

Figure 8: Simulating of avalanche probability.

PoS(PD09)003

The current structure of MPPC is shown in Figure 7. For most field structures, the multiplication region is localized within the depletion layer while carriers simply drift in the greater part of the depletion layer. The impact ionization coefficient for electrons is roughly one order of magnitude higher than that for holes at the region where the strength of the electric field is a few hundred kV/cm [4]. The geometry of the device is critical in explaining the disparity in the voltage dependence between the carriers. Given that the absorption length for 470 nm wavelength is 0.5 μm [5], the photoelectric conversions occur mostly near the top surface. The charge carriers which undergo multiplication in this case is the electron. On the other hand, random excitations occur throughout the bulk of the device. Since the n-side is larger in volume, the holes are the dominant carriers in this case. The difference in the voltage dependence can be thus explained in terms of the difference in charge carriers. Based on these ideas, we performed a MC simulation to estimate the voltage dependence of the avalanche probability for electrons and holes separately. We find that the avalanche probability for electrons is higher and saturates as the bias voltage increases, as shown in Figure 8. The measured noise rate as the bias voltage increases [2] resembles the measured relative PDE. These ideas can explain the difference in the voltage dependence between the random noise and the PDE.

3. Status Report of Simulation

3.1 Technology Computer Aided Design

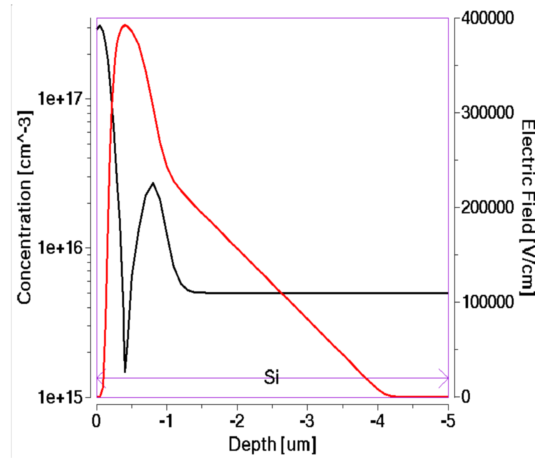

Figure 9: Simulated electric field (red) and dopant concentration (black).

We report the current application status of the device simulator in three dimension using TCAD which is called “ENEXSS" made by TCAD International, Inc. A design structure is divided using a mesh. The finite difference method is employed to solve the device equations with specified boundary conditions to obtain the device characteristics. Static and transient analyses can be both performed. The present phase in our research is to evaluate the potential of TCAD for the development of PPD. We tried to reproduce the breakdown phenomenon and the avalanche multiplication in the simulation of a PN-diode. The PN-diode is a p-on-n type diode whose profile is built using the impurity concentration distribution of SiPM (Silicon Photomultiplier) made by ITC-irst [6] as shown in Figure 9. The P-side is doped with Boron. The N-side is doped with Phosphorus.

3.2 Breakdown Voltage

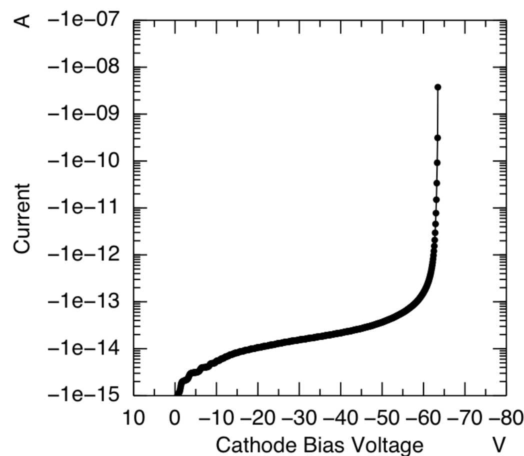

Figure 10: Simulated IV-curve of an PPD in static analysis

PoS(PD09)003

We first perform a static analysis of the device under a reverse bias. In Figure 10, the anode current is shown as a function of the bias voltage. We find a current shoot-up around -63 V which is due to the impact ionization model. We have reproduced the breakdown voltage phenomenon.

3.3 Avalanche multiplication

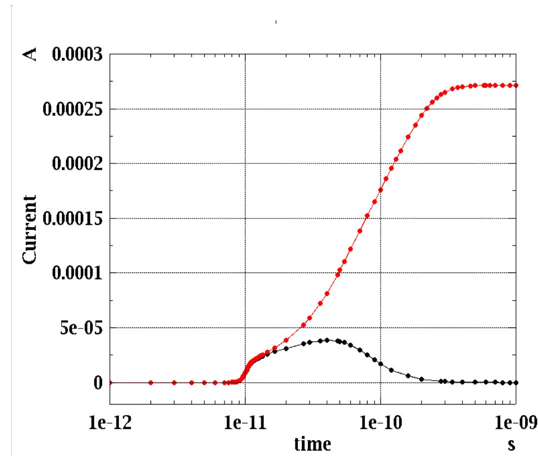

Figure 11: Simulated avalanche multiplication in transient analysis (for the detail, see text.).

We are interested in the avalanche multiplication process because we want to reproduce the quenching mechanism in the future. Transient analysis is essential in this aim. Since we already know from the static analysis that the breakdown occurs around -63 V, a transient analysis was performed around this voltage.

As seen above, we simulated the multiplication process of the PN-diode in transient analysis. Additionally, we create an electron-hole pair inside the device, corresponding to thermal excitation or an incident photon. Figure 11 shows the simulation results of the avalanche multiplication. These plots show the anode current as a function of time. The black curve shows the result with the operational voltage of -60 V, which is below the breakdown voltage. The current temporarily increases, which then decreases gradually. On the other hand, the red curve shows the result with the operational voltage of -65 V, which is above the breakdown voltage. The current grows drastically and the avalanche multiplication does occur. As a result, we confirmed that the avalanche multiplication occurs between -60 V and -64 V, which is close to the breakdown voltage.

4. Conclusion

We measured and understood the three noise components separately. The voltage dependence of the random noise rate is mostly linear. The total noise rate is fully accounted for by the combination of random noise, after-pulse, and crosstalk. The voltage dependence of the random noise and PDE was understood in terms of the charge carriers. Using TCAD, we successfully reproduced the breakdown voltage phenomenon and the avalanche multiplication. In the future, work is needed for better agreement between data and simulation. We plan to reproduce the quenching mechanism and make progress toward obtaining a new PPD design.

PoS(PD09)003

5. Acknowledgment

The authors wish to express our deep gratitude to the KEK-DTP photon-sensor group members for helpful discussions and suggestions. This work was supported by Grant-in-Aid for Exploratory Research 20654021 from the Japan Society for the Promotion of Science (JSPS), Creative Scientific Research 18GS0202, by Grant-in-Aid for JSPS Fellows 20.4439, and 21.7995.

References

[1] Hamamatsu Photonics K.K.(http://jp.hamamatsu.com/products/sensor-ssd/4010/4025/)

[2] H. Oide , et al., "Studies on multiplication effect of noises of PPDs, and a proposal of a new structure to improve the performance", NIMA (http://arxiv.org/abs/0811.1402)

[3] S. Uozumi, et al., "Development and study of the multi pixel photon counter", NIMA 581 (2007) 427-432

[4] W Maes, K De Meyer, and R Vanonerstraeten. Impact Ionization in Silicon - A Review and Update. Solid State Electron, Vol. 33, No. 6, pp. 705-718, Jan 1990.

[5] WC Dash and R Newman. Intrinsic Optical Absorption in Single-Crystal Germanium and Silicon at 77-Degrees-K and 300-Degrees-K. Phys Rev, Vol. 99, No. 4, pp.1151-1155, Jan 1955.

[6] Claudio Piemonte. A New Silicon Photomultiplier Structure for Blue Light Detection. NIMA, Vol.568, No.1, pp. 224-232, Nov 2006.

PoS(PD09)003